Journal of Theoretical and Applied Information Technology
31st July 2020. Vol.98. No 14

ISSN: 1992-8645 www.jatit.org E-ISSN: 1817-3195

CONTROL OF AN AUTONOMOUS PV SYSTEM USING THE BACKSTEPPING MPPT CONTROLLER UNDER REAL CLIMATIC CONDITIONS IN NORTHERN MOROCCO

[1]HANANE YATIMI, [2]YOUNESS OUBERRI, [3]RIM MARAH, [4]ELHASSAN AROUDAM

[1,2,4]Modeling and Simulation of Mechanical Systems Team, Department of Physics, Faculty of Sciences, Abdelmalek Essaadi University, Tetouan, Morocco

[1,3]Systems, Control & Decision Laboratory, Ensit Engineering School, Tangier, Morocco

[3]Computer Science and Systems Engineering Laboratory, Faculty of Sciences, Abdelmalek Essaadi University, Tetouan, Morocco

E-mail: [1]yatimi.hanane@gmail.com, [2]ouberriyouness@gmail.com, [3]ensate.rim@gmail.com, [4]aroudam_hass@hotmail.com

ABSTRACT

Maximum power point tracking (MPPT) methods are widely used with PV solar systems to maximize power extraction under variants whether conditions. On another hand the system stability around the maximum power point depends on the robustness of the used method for better load charging conditions. This paper presents a non-linear backstepping controller, based on the Lyapunov function, and applied to an autonomous PV system as a MPPT controller, to extract its maximum power, under simultaneous changes in solar radiation and temperature. A DC-DC boost converter is used as a bridge between the PV module and the load. To validate the robustness of the proposed backstepping controller, the system outcomes under variant meteorological conditions using both the backstepping controller and the well-known incremental conductance method are compared. The results based on analyzing and interpreting the power, voltage and current curves and system behavior, reveal that by using the backstepping controller, the asymptotic stability of the system is smoothly guaranteed with practically no oscillation around the maximum power point and far exceeds the incremental conductance performance in terms of speed and accuracy.

Keywords: *Photovoltaic (PV), Maximum Power Point Tracking (MPPT), Boost Converter, Backstepping Controller (BSC), Recursive Structure*

1. INTRODUCTION

Nowadays, the electricity production using fossil energy resources (oil, gas…) leads to the depletion of its reserves and intensifies the release of greenhouse gases and thus the pollution of the atmosphere resulting climate change. Faced with these alarming consequences, it was necessary to consider the development of alternative energy called renewable energy sources. These sources are the best available options to fulfill the demand of power. Amongst these, photovoltaic solar energy receives great attention because it is relatively less polluted and maintenance, an inexhaustible source, free and superabundant, very promising, available in every country and every day [1, 2]. It is widely used in many applications such as solar vehicle construction, water pumping [3, 4], satellite power systems, battery charging, and so on. Unfortunately, PV systems have some problems: in fact, the sun doesn't shine 24 h a day, when the sun goes down or is heavily shaded, solar PV panels stop producing electricity. In addition, solar energy conversion efficiency into electrical energy is very low especially in low radiation areas, and changes with environmental conditions such as solar radiation, atmospheric temperature and also nature of connected load [2]. Moreover, a PV module has non-linear relation-ship between the current and the voltage and generated power depends on the aforementioned environment conditions. To increase the efficiency of the PV system, it is crucial to operate the PV energy conversion systems near the maximum power point [5].

ISSN: 1992-8645 www.jatit.org E-ISSN: 1817-3195

Therefore, MPPT are essential to track the MPP of the system. Thus, the use of these trackers plays an important role in increasing the conversion efficiency as well as decreasing the cost of a PV system [6].

In recent times, intensive research work is being done in this particular field to strive for robust and more efficient MPPT controllers. So, there are many techniques available in the literature such as the Perturb and Observe (P&O) technique [7, 8], which is the most commonly used for extracting maximum power from PV module due to its simplicity. However, this technique has several limitations, such as, continuous oscillations around the operating point and poor tracking result or slower convergence speed [6]. For this issue, many methods have been proposed to improve the efficiency of the P&O for MPPT by reducing the steady state oscillation and eliminating the possibility of losing the tracking direction. For example [9-12], have made a comparison between the conventional and the proposed adaptive P&O techniques to highlight first, the weak side of the classical P&O technique regarding the oscillation around the MPP and then discuss the improved one, which reduce but not illuminate the oscillation issue. The Incremental Conductance (IC) technique [13, 14] overcomes the drawbacks of the P&O technique by giving faster convergence speed under variable climatic conditions, but requires complex control circuit and the oscillation matter around the MPP still present. On the other hand, the main issue with the IC technique is that during the increment of solar irradiance, the conventional one responds inaccurately at the first step change in the converter duty cycle. So, like P&O technique, IC technique needs to be improved. [15, 16], Propose a modified incremental conductance algorithm that responds accurately when large changes occur in the irradiance, the outcomes of the modified methods are largely better compared to classical one, but the problem of oscillation persist.

The Fuzzy Logic Control search technique (FLC) [17], which is used very successfully in the implementation for MPP searching, improves control robustness. In fact, FLC does not require exact mathematical models, can handle non-linearity, and gives robust performance under parameters and load variations. In [18], the robustness of the FLC was challenged by comparing the results obtained from the experimental investigation with the simulation studies results of the three-phase grid-connected photovoltaic systems and it has been found that the simulation results closely agree with the experimental obtained results, thus validating demonstrate that the FLC is one of the best available controllers of the MPP. The main problem with the fuzzy logic controllers is that they requires expert knowledge of the process operation for FLC parameter setting, and the controller can be only as good as the expertise involved in the design [19]. The Artificial Neural Network (ANN) based MPPT technique is also used to track the MPP of the PV module with success thanks to its low computation requirement and fast tracking speed [20].

Recently, numerous researches are being carried out in the area of nonlinear control. There are many nonlinear MPPT controllers in the literature for tracking the MPP of PV module, such as Sliding Mode Controller [21-23]. The SMC provides robust performance against the parameter variations and external disturbances; it can reach the steady state of different irradiance levels within the order of milliseconds, which is much faster compared to the other MPPT tracking techniques such as P&O and IC [24]. In [22], the SMC is proposed to improve the quality of the produced power of a PV module, the Lyapunov function is used to ensure the stability of the system. To be noted that the chattering phenomenon is still a shortcoming of this technique.

In this research paper, in order to overcome all aforementioned limitations of the linear controllers, a new nonlinear controller for MPPT is designed. It is independent of operating points and has the ability of providing satisfactory operation under changing atmospheric conditions [25]. A nonlinear backstepping controller; of the switching period of a boost converter; is proposed. The global asymptotic stability is guaranteed by means of Lyapunov stability function and the MPP is reached even in changeable environmental conditions. The advantages of backstepping controllers are related to the use of the converters model direct dynamics, and Lyapunov functions to guarantee the stability and robustness of the system [26, 27].The paper is organized as follows: Section 2 describes the modeling of PV system components, including the mathematical representation of the PM module, the DC/DC boost converter and the DC load. The proposed controller design and a brief presentation of the conventional incremental conductance MPPT controller are provided in Sections 3 and 4, respectively. Section 5 shows and discusses the obtained results. Finally, conclusions are addressed in Section 6.

Journal of Theoretical and Applied Information Technology
31st July 2020. Vol.98. No 14

ISSN: 1992-8645 www.jatit.org E-ISSN: 1817-3195

2. MODELING OF PV SYSTEM COMPONENTS

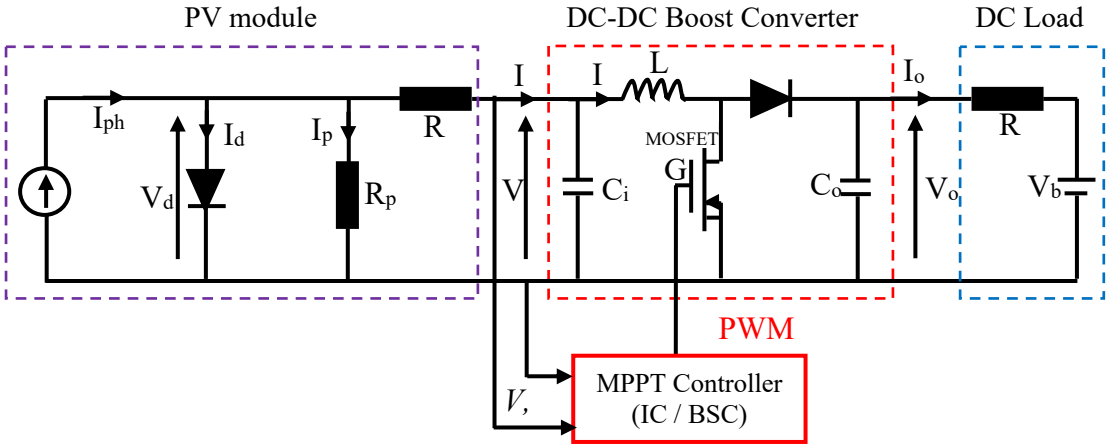

Figure 1: The schematic of PV system.

The considered PV system is mainly consisting of a PV module, DC-DC boost converter, control system (MPPT tracker) and a DC load as shown in Fig. 1. In this system, the MPP tracker is used to maintain a constant PV module output voltage and the proposed control method will ensure the convergence of this voltage to its desired value. To achieve this, the boost converter must operate with a specific duty cycle that yields to the maximum power. So, the sizing of the boost converter is essential.

2.1 PV Module

The PV module is composed of group of cells; its model is based on that of a PV cell, associated in series and/or parallel. The PV cell is modeled as an equivalent circuit [28, 29]. This model consists of an ideal current source I_{ph} in parallel with a diode and R_p all in series with resistor R_s as shown in Fig. 1. The diode models the semiconductor material, and R_s models the resistance between the contactor and the semiconductor material. The output current–voltage characteristic of a PV module is given by the following equation [30]:

$$I = N_p I_{ph} - N_p I_0 \left[\exp\left(\left(\frac{q}{akT} \right) \left(\frac{V}{N_s} + \frac{IR_S}{N_p} \right) \right) - 1 \right] - \frac{N_p}{R_{sh}} \left(\frac{V}{N_s} + \frac{IR_s}{N_p} \right) \quad (1)$$

Where, N_s and N_p are the series and the parallel solar cell per module, respectively.
I_{ph}: is the generated photocurrent (A), it is expressed as,

$$I_{ph} = \left[I_{scr} + K_i \left(T - T_r \right) \right] \left(\frac{G}{1000} \right) \quad (2)$$

I_0: is the reverse saturation current of diode (A), it is influenced by the temperature according to the following equation,

$$I_0 = I_{rs} \left[\frac{T}{T_r} \right]^3 \exp\left[\left(\frac{qE_{g_0}}{aK} \right) \left(\frac{1}{T_r} - \frac{1}{T} \right) \right] \quad (3)$$

Where V, I, I_{scr}, I_{rs}, K_i, q, K, a, T_r, T, G, R_s and R_p refer to PV module output voltage, PV module output current, short-circuit current at reference condition, saturation current at reference temperature, short-circuit temperature coefficient, electron charge ($1.60217.10^{-19}$ C), Boltzmann constant ($1.38.10^{-23}$ J/K), diode ideality factor, reference temperature (K), PV cell Temperature (K), solar radiation (W/m^2), series resistance of PV cell (Ω), parallel resistance of PV cell (Ω), respectively. R_s: mainly due to losses by Joule effect through grids collection and to the specific resistance of the semiconductor, as well as bad contacts (semi conductor, electrodes). R_p: Parallel resistance comes from the recombination losses mainly due to the thickness, the surface effects and the non-ideality of the junction. The PV cell temperature is depending on ambient temperature and solar radiation, it is given by:

$$T = T_{Amb} + \left(NOCT - 20°C \right) \left(\frac{G}{800} \right) \quad (4)$$

ISSN: 1992-8645 www.jatit.org E-ISSN: 1817-3195

The output power of the PV module can be given explicitly as follows:

$$P = V \times I = V \times \left\{ N_p I_{ph} - N_p I_0 \left[\exp\left(\left(\frac{q}{akT} \right) \left(\frac{V}{N_s} + \frac{IR_S}{N_p} \right) \right) - 1 \right] - \frac{N_p}{R_{sh}} \left(\frac{V}{N_s} + \frac{IR_s}{N_p} \right) \right\} \quad (5)$$

2.2 Effects of Climatic Conditions on PV Module Characteristics

2.2.2 Meteorological data-sets

The real meteorological data locally measured at regular intervals (1 hour) throughout the typical clear day of January in Tetouan (Northern Morocco), from sunrise to sunset are given by Figs. 2 and 3. The important statistics of the used meteorological data are presented in Table 1. To sum up, the use of the MPPT techniques to extract the maximum available power at any changes is primordial.

Table 1 : Important statistics of the daily data-set measured from experimental setup used in this paper.

January 24, 2015			
LTD (hour)	G (maximum) (W/m²)	Ambient Temperature (°C)	Cell's Temperature (°C)
8:00	10.83333	6.7	7.35
9:00	45.83333	9.4	12.149
10:00	335.27778	13.5	33.62
11:00	513.05556	14.6	45.38
12:00	602.50000	15.6	51.75
13:00	632.77778	16.3	54.26
14:00	606.66667	17.2	53.6
15:00	502.22222	16.8	46.93
16:00	350.00000	15.3	36.3
17:00	163.05556	14.2	23.98
18:00	12.77778	11.9	12.68

LTD: Local Time of Day. G: solar irradiance.

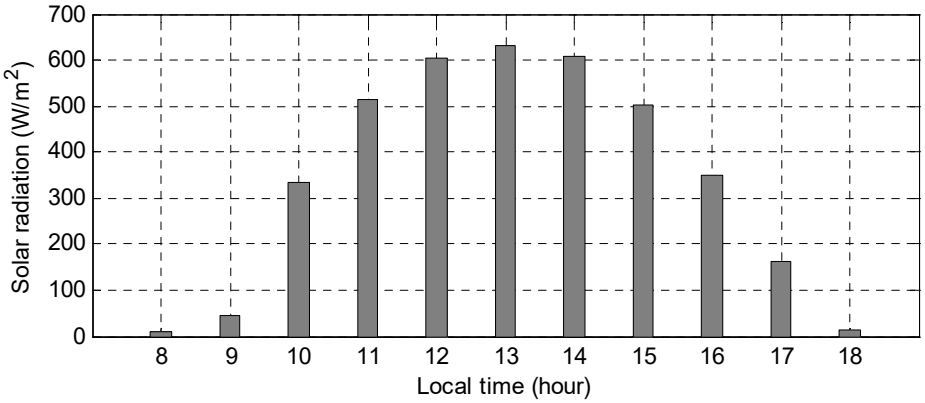

Figure 2: Time dependences of solar radiation measured in the typical clear day of January (2015).

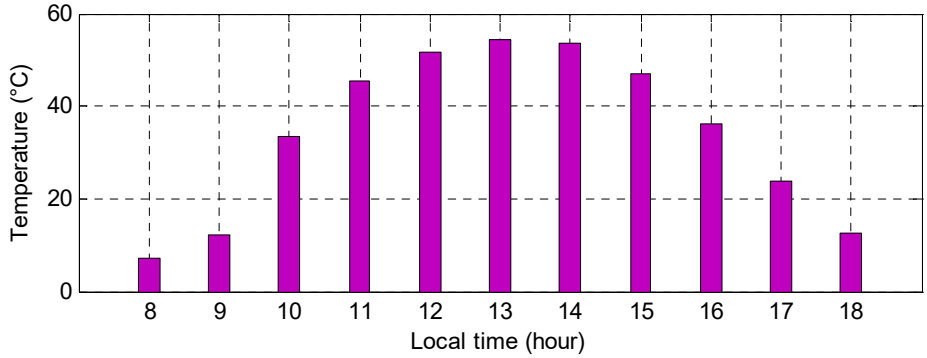

Figure 3: Time dependences of temperature measured in the typical clear day of January (2015).

ISSN: 1992-8645 www.jatit.org E-ISSN: 1817-3195

2.2.3 Current-voltage and power-voltage characteristics at constant temperature and variable solar radiation

Fig 4 shows the behavior of the used PV module under the effect of solar radiation variation and constant temperature equals to 25 °C, considering an example of one month of winter (January, 2015). From these curves, it can be seen that solar radiation has a significant effect on the short-circuit current, while the effect on the voltage in open circuit is quite low. Regarding the power, as seen in the figure, it increases during the first hours of the day and gradually decreases and the existence of the maximum on the power curves is clearly noticed, corresponding to the Maximum Power Point P_{MPP}.

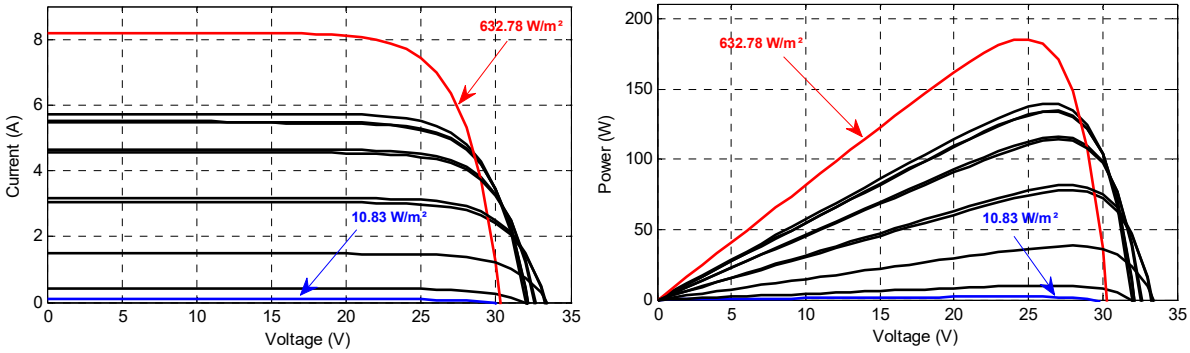

Figure 4: Current-voltage and power-voltage characteristics at constant temperature and variable solar radiation for the typical clear day of January (2015) - Tetouan/Morocco.

2.2.4 Current-voltage and power-voltage characteristics at constant solar irradiance and variable temperature

Fig. 5 shows the behavior of a PV module under the effect of temperature variation and constant solar radiation equals to 1000 W/m^2, considering an example of one month of winter (January, 2015). From these curves, it can be clearly detected that the temperature has a very important effect on the open circuit voltage and no remarkable effect on both the short circuit current and the power of the module.

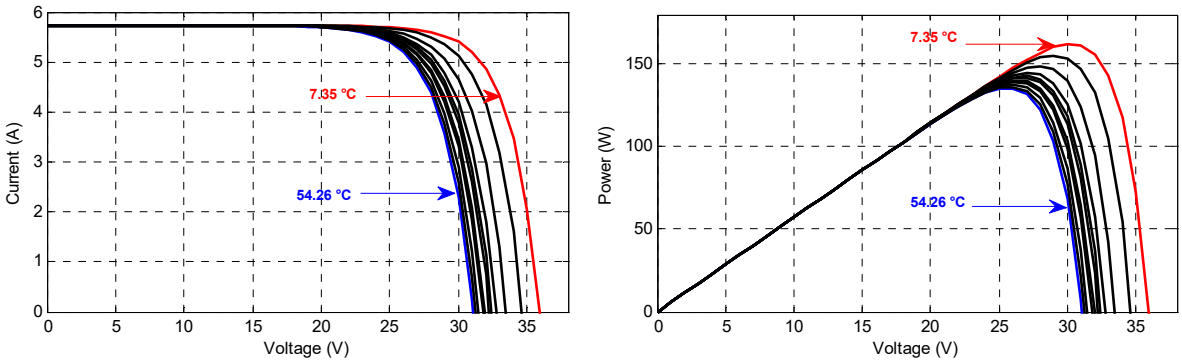

Figure 5: Current-voltage and power-voltage characteristics at variable temperature and constant solar radiation for the typical clear day of January (2015) - Tetouan/Morocco.

2.3 DC-DC Boost Converter and Battery

The boost converter is a DC-to-DC power electronic converter steps up voltage (while stepping down current) from its input to its output. If the chopping frequency is sufficiently higher than the system characteristic frequencies, the converter can be replaced with an equivalent continuous model as shown in Fig. 1. And the mean values of the electric quantities, over the chopping period will be considered. The considered boost converter is consists of two switches (diode and transistor), an inductor, capacitors, and one energy storage element which is represented by a simple voltage

ISSN: 1992-8645 www.jatit.org E-ISSN: 1817-3195

source V_b in series with a resistor R_b. It's operates in continuous conduction mode with an input filter (Ci, L) and an output filter Co. It's controlled periodically with a modulation period T. Over this period, t_{on} is called the closing time and t_{off} is the opening time, $T = t_{on}+t_{off}$. The duty cycle of the converter is defined as, $\alpha = t_{on}/T$. The switches are alternatively opened and closed. Considering the periods of open and closed circuit operation, the state equations of the boost converter average model [31] operating in continuous conduction mode are:

$$\begin{cases} \frac{dV}{dt} = \frac{I}{C_i} - \frac{I_L}{C_i} \\ \frac{dI_L}{dt} = \frac{V}{L} - \frac{(1-\alpha)}{L} V_o \\ \frac{dV_o}{dt} = \frac{V_o}{C_o R_b} - \frac{V_b}{C_o R_b} + \frac{(1-\alpha)}{C_o} I_L \end{cases} \quad (6)$$

Where:

$$V_o = V_b + R_b I_o \quad (7)$$

I and V are the output current and voltage of the PV module, I_L is the inductor current, I_o *and* V_b are the average states of respectively the battery current and the battery voltage, V_o is the DC/DC converter output voltage, α is the duty cycle, which represents the control input, L is the DC/DC converter inductance and C_i and C_o are respectively the input capacitor and the output capacitor of the converter.

3. PROPOSED NONLINEAR CONTROLLER DESIGN

In order to charge the battery with the maximum power, the suggested techniques compel the system to run to its optimal operating point under varying climatic conditions. The main role of these MPPT controllers is to modify the duty cycle of the boost converter until reaching the MPP of the system.

The global mathematical model of the nonlinear studied system in state space is given by:

$$\begin{cases} \frac{dx_1}{dt} = \frac{I}{C_i} - \frac{1}{C_i} x_2 \\ \frac{dx_2}{dt} = \frac{1}{L} x_1 - \frac{u}{L} x_3 \\ \frac{dx_3}{dt} = \frac{V_b}{C_o R_b} + \frac{1}{C_o R_b} x_3 + \frac{u}{C_o} x_2 \end{cases} \quad (8)$$

Where,

$$x_1 = V;\ x_2 = I_L;\ x_3 = V_o;\ u = 1-\alpha;\ y = \frac{\partial P}{\partial V}$$

From the power-voltage characteristic curves of Fig. 4 and 5, the PV module power is maximal when its derivative with respect to its voltage is equal to zero.

- *Backstepping control and stability analysis*

The backstepping controller is a recursive design methodology. It involves a systematic construction of both feedback control laws and associated Lyapunov functions. The controller design is performed in a number of steps which is equals to the system order. The main aim of this controller is to determine the maximum power operating point by tracking a desired module voltage which can be achieved by modulating the pulse width of the switch control signal (increasing or decreasing the duty ratio of the switching converter). The system output to be controlled is given by:

$$y = \frac{\partial P}{\partial V} \quad (9)$$

The relative degree r = 2 of the studied system corresponds to the number of times the output y has to be differentiated with respect to time before the command u appears explicitly in the resulting equations. We have the first and second time derivative of the controlled output y, after the second derivation of the output of the system the following expression is obtained:

$$\ddot{y} = \frac{\partial^2 P}{\partial t^2} = H_1(x,t) + H_2(x,t)u \quad (10)$$

With

$$H_2(x,t) = \frac{1}{C_i}\left(\frac{\partial^2 P}{\partial V^2}\right)\frac{V_o}{L} \quad (11)$$

ISSN: 1992-8645 www.jatit.org E-ISSN: 1817-3195

$$H_1(x,t)=\left(\frac{\partial^3 P}{\partial V^3}\right)\left(\frac{\partial V}{\partial t}\right)^2+\frac{1}{C_i}\left(\frac{\partial^2 P}{\partial V^2}\right)\left[\left(\frac{\partial I}{\partial V}\right)\left(\frac{\partial V}{\partial t}\right)-\frac{V}{L}\right] \quad (12)$$

Backstepping design procedure: as the system order is equal to 2, the design of the control can be obtained in two steps.

Steps 1: First of all we define the tracking error:

$$\varepsilon_1 = y - y_d \quad \text{with} \quad y_d = 0\,. \quad (13)$$

Where y_d is the desired value of the system output y. By converging the ε1 to zero, the desired result will be obtained. Taking the derivative of Eq. (13), we have the first subsystem:

$$d\varepsilon_1 = dy = \frac{1}{C_i}\left(V\frac{\partial^2 I}{\partial^2 V}+2\frac{\partial I}{\partial V}\right)\left(I - I_L\right) \quad (14)$$

The stabilization of ε_1 can be obtained by introducing a new virtual control input:

$$\alpha_1 = d\varepsilon_1 = dy \quad (15)$$

Considering the first Lyapunov function V_1 to check the convergence of the error ε1 to equilibrium point.

$$V_1(\varepsilon_1)=\frac{1}{2}\varepsilon_1{}^2 \quad (16)$$

The Lyapunov function must be positive definite and its derivative with respect to time must be negative definite, so that the asymptotic stability is guaranteed [29]. The time derivative of Eq. (16) is given by:

$$dV_1 = \varepsilon_1 . d\varepsilon_1 = \varepsilon_1 . \left[\frac{1}{C_i}\left(V\frac{\partial^2 I}{\partial^2 V}+2\frac{\partial I}{\partial V}\right)\left(I - I_L\right)\right] = -b_1\varepsilon_1^2 < 0 \quad (17)$$

The virtual control law would be:

$$\alpha_1 = -b_1\varepsilon_1 \quad (18)$$

where b_1 is a positive gain.

Steps 2: Let us put:

$$\varepsilon_2 = \frac{dy}{dt} - \alpha_1 \quad (19)$$

Taking the derivative of Eq. (19) with respect to time, the second subsystem can be written as:

$$\frac{d\varepsilon_2}{dt} = \frac{d^2 y}{dt^2} + \frac{d\alpha_1}{dt} \quad (20)$$

Substituting Eq. (19) into Eq. (15), $d\varepsilon_1$ becomes:

$$\frac{d\varepsilon_1}{dt} = \varepsilon_2 + \alpha_1 \quad (21)$$

Introducing Eqs.(18) and (21) in Eq. (17), we obtain:

$$\frac{dV_1}{dt} = -b_1\varepsilon_1^2 + \varepsilon_2\varepsilon_1 \quad (22)$$

The composite Lyapunov function must be positive definite and its derivative with respect to time must be negative definite, in order to insure the asymptotic stability of the system and then to insure the convergence of the two errors (ε1 and ε2) to zero.

$$V_2 = V_1 + \frac{1}{2}\varepsilon_2{}^2 \quad (23)$$

Its time derivative is:

$$\frac{dV_2}{dt} = \frac{dV_1}{dt} + \varepsilon_2\frac{d\varepsilon_2}{dt} \quad (24)$$

The combination of (10), (20), (22) and (24) gives:

$$u = \frac{\left(-b_2\varepsilon_2 - \varepsilon_1 - H_1 + {d\alpha_1}/{dt}\right)}{H_2} \quad (25)$$

Where b_2 is a positive gain.

Substituting Eqs. (11) and (12) into Eq. (25), we get:

$$u = \frac{\left(-b_2\varepsilon_2 - \varepsilon_1 - \left(\left(\frac{\partial^3 P}{\partial V^3}\right)\left(\frac{\partial V}{\partial t}\right)^2+\frac{1}{C_i}\left(\frac{\partial^2 P}{\partial V^2}\right)\left[\left(\frac{\partial I}{\partial V}\right)\left(\frac{\partial V}{\partial t}\right)-\frac{V}{L}\right]\right) + d\alpha_1\right)}{\left(\frac{1}{C_i}\left(\frac{\partial^2 P}{\partial V^2}\right)\frac{V_o}{L}\right)} \quad (26)$$

Which means that ε_1 and ε_2 converge asymptotically to the origin, which implies that $y = \partial P/\partial V$ converges asymptotically to the origin

Journal of Theoretical and Applied Information Technology
31st July 2020. Vol.98. No 14

ISSN: 1992-8645 www.jatit.org E-ISSN: 1817-3195

(desired value y_d), fulfilling the tracking control objective. Therefore, the output power tracks the MPP of photovoltaic module.

Fig. 6 depicts a flow chart in order to summarize the design of the backstepping controller. The steps described in this flow chart are translated into a script file in Matlab IDE.

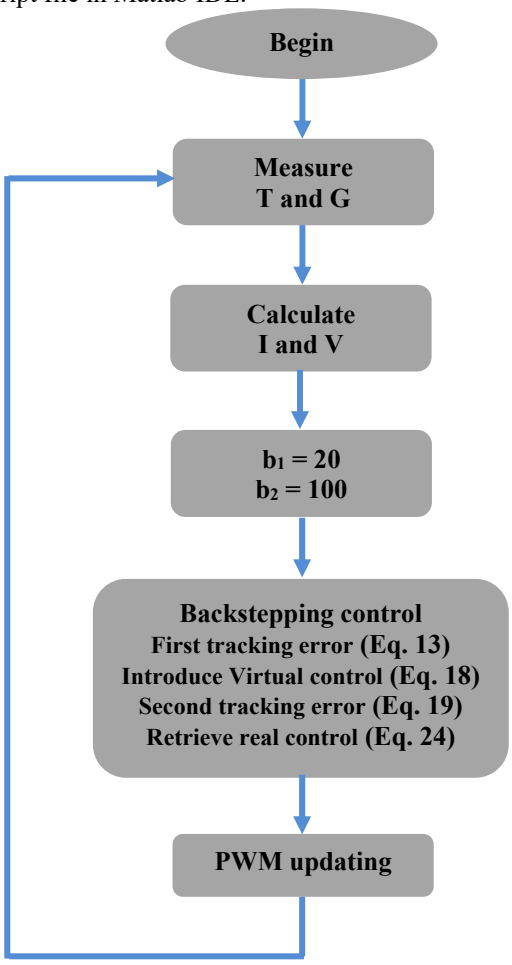

Figure 6: Backstepping controller flow chart.

4. CONVENTIONAL MPPT ALGORITHM

The Incremental Conductance (IC) algorithm is based on the fact that the P-V curve of a PV module has only one MPP (Fig. 7). The output power of PV module can be expressed as: $P=V\times I$ .Then the derivative of product yields:

$$\frac{dP}{dV}=\frac{d(V.I)}{dV}=I+V.\frac{dI}{dV} \quad (27)$$

Where, P, V and I are the PV module output power, voltage and current, respectively. The slop of the PV module power-voltage curve (dP/dV) equals to zero at the MPP, increasing on the left of the MPP and decreasing on the right side of the MPP [32], which is expressed by the following equations:

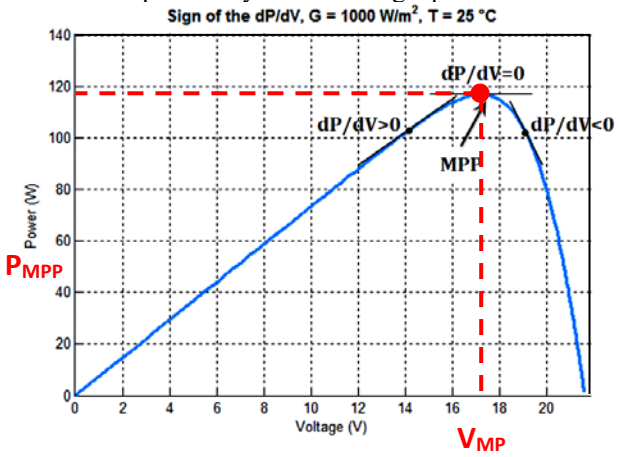

Figure 7: Sign of the dP/dV at different positions on the P-V characteristic curve of a PV module.

$$\begin{cases}\frac{dP}{dV}=0\Rightarrow\frac{dI}{dV}=-\frac{I}{V}, & at\ MPPT\\ \frac{dP}{dV}>0\Rightarrow\frac{dI}{dV}>-\frac{I}{V}, & left\ of\ MPPT\\ \frac{dP}{dV}<0\Rightarrow\frac{dI}{dV}<-\frac{I}{V}, & right\ of\ MPPT\end{cases} \quad (28)$$

These equations are used to determine the direction in which a perturbation must occur to shift the operating point toward the MPP and the perturbation is repeated until $^{dP}/_{dV}=0$.

To sum up, this algorithm requires the values of the PV module output current and voltage to calculate the conductance and the incremental conductance. The operating point tracks MPP by comparing the immediate conductance (I/V) to the Incremental Conductance (dI/dV). Once, the MPP is reached, the operation of the PV module is maintained at this point unless a change in dI is noticed, indicating a change in meteorological conditions. Main steps of this MPPT algorithm are depicted with the help of the flowchart of Fig. 8.

5. SIMULATION RESULTS AND DISCUSSIONS

The performance of the proposed controller is verified by numerical simulation. PV module has been connected to the load through boost converter controlled by the backstepping controller. The whole system is implemented in Matlab/Simulink environment (Fig. 9) under the simultaneous variation of the solar radiation and temperature (Table 1).

ISSN: 1992-8645 www.jatit.org E-ISSN: 1817-3195

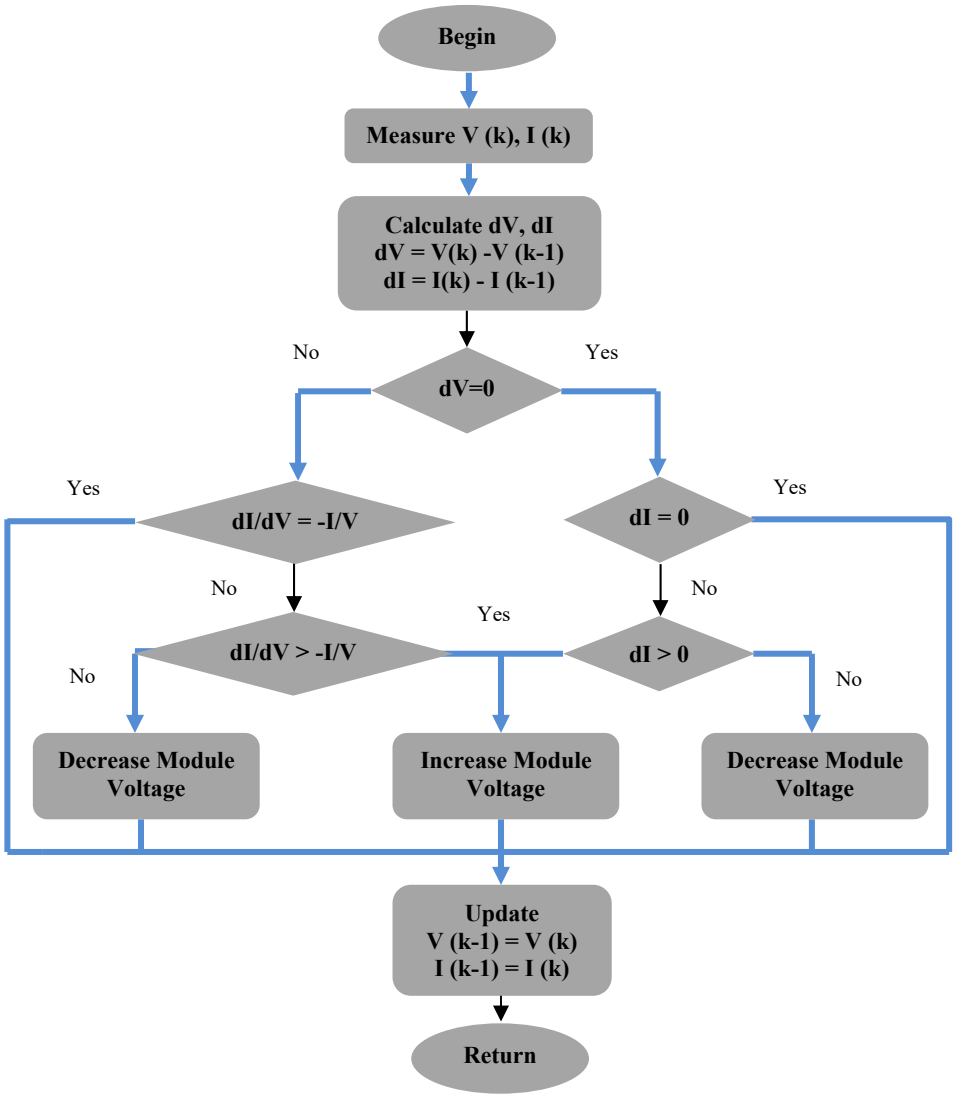

Figure 8: The conventional Incremental Conductance Flowchart.

The PV module used in this work consists of 60 PV cells connected in series i.e. $N_p = 1$. Its electrical specifications are shown in Table 2, whereas the specifications of the controller and the boost converter are shown in Table 3.

To test the effectiveness of the proposed MPPT controller whatever the change of weather conditions, the real measurement of solar radiation and temperature of the typical clear day of one month of the winter (January, 08.00 am-06.00 pm) has been considered. The varying levels of both solar radiation and temperature are shown in Fig. 10. Initial radiation is 10.83 W/m², and then it is hourly increased to 45.83 W/m², 335.28 W/m², 513.06 W/m², 602.50 W/m² until achieve its maximal value 632.78 W/m² at 01.00 pm. From this time, the solar radiation witnessed a decrease back to 606.67 W/m², and it is still hourly decreasing to 502.22 W/m², 350 W/m², 163.06 W/m², and 12.78 W/m². Simultaneously, Initial ambient temperature is 6.7 °C, and then it is hourly increased to 9.4 °C, 13.5 °C, 14.6 °C, 15.6 °C, 16.3 °C until achieve its maximal value 17.2 °C at 02.00 pm. From this time, the ambient temperature witnessed a decrease back to 16.8 °C, and it is still hourly decreasing to 15.3 °C, 14.2 °C and 11.9 °C.

Fig. 11-a depicts the output power of the PV module with MPPT scheme at eleven levels of solar radiation and temperature. It is clearly seen that the IC MPPT technique catch the MPP whatever the change of solar radiation and temperature. But it still takes considerable amount of time to reach MPP in addition to the oscillation around it (Fig. 11-b), which results to the energy losses.

ISSN: 1992-8645 www.jatit.org E-ISSN: 1817-3195

Table 2 : PV module parameters.

Parameter	Description	Value	Unit
N_s	Number of cells in series per module	60	-
P_{max}	Maximum power	255	W
V_{mp}	Voltage at MPP	30.6	V
I_{mp}	Current at MPP	8.43	A
V_{oc}	Open circuit voltage	38.7	V
I_{sc}	Short circuit current	9.05	A
K_i	Temperature coefficient for Isc	0.044	%/K
$NOCT$	Nominal Operating condition Temperature	48	°C
R_s	Series resistance	309	mΩ
R_{sh}	Parallel resistance	6.5	kΩ
a	Ideality factor	1.3257	-
I_{SCR}	Short circuit current at STC	9.0504	A
I_{rs}	Saturation current at T_r	[1] 54.389	nA
T_r	Reference temperature	298.15	K

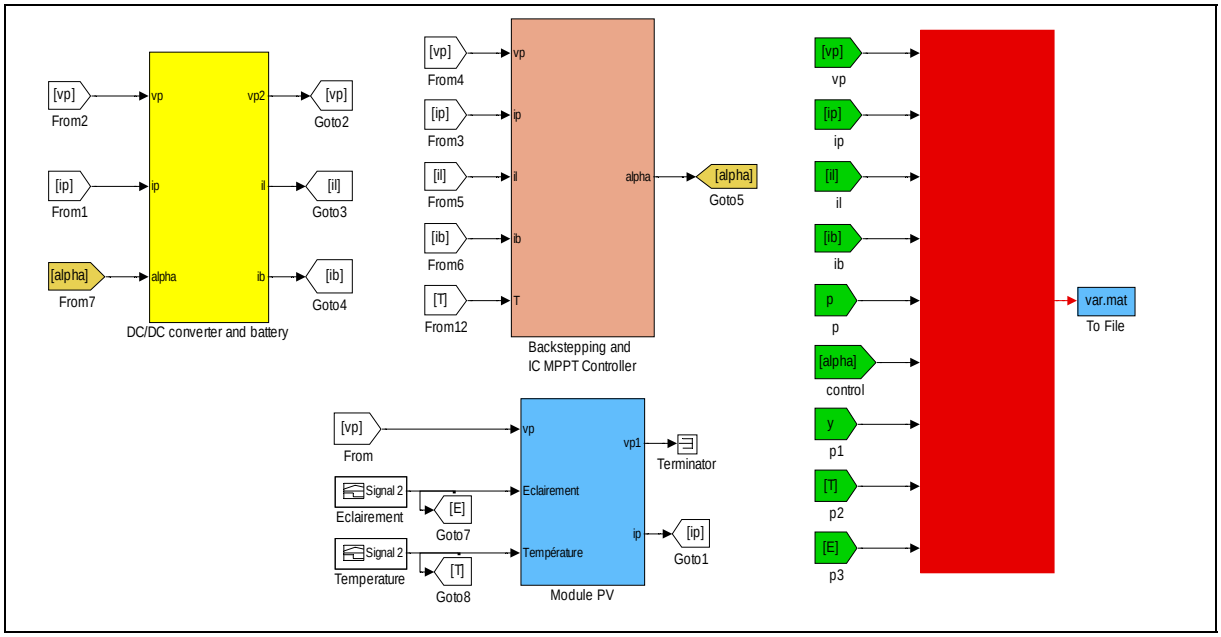

Figure 9: Block diagram model of the proposed PV system on Matlab/Simulink.

Table 3:Simulation parameters.

Parameter	Name	Value	Unit
Controller parameters			
b1	Constant	20	-
b2	Constant	100	-
DC-DC converter			
L	Inductance	2.2	mH
C_i	Input capacitor	47	mF
C_b	Output capacitor	4.7	mF
DC Load			
V_b	Battery voltage	48	V
R_b	Battery resistance	2	Ω

ISSN: 1992-8645 www.jatit.org E-ISSN: 1817-3195

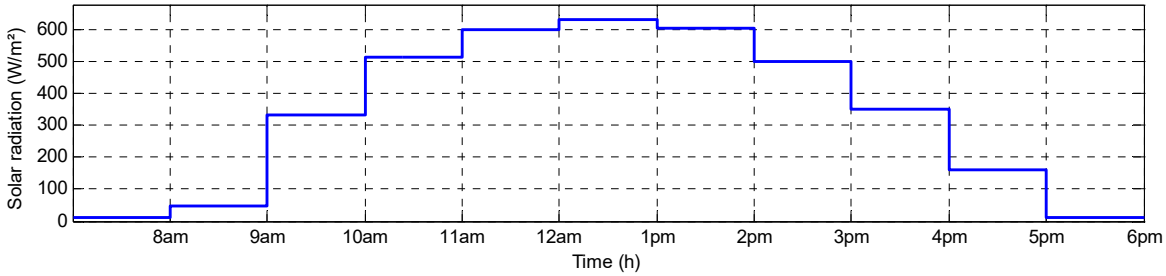

Figure 10-a: Varying levels of solar radiation.

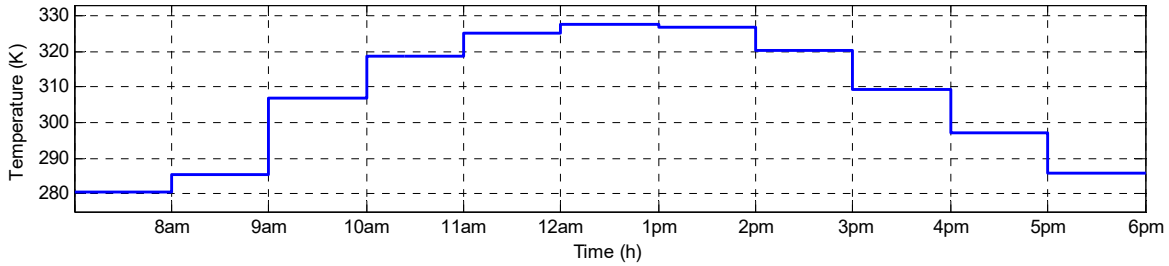

Figure 10-b: Varying levels of temperature.

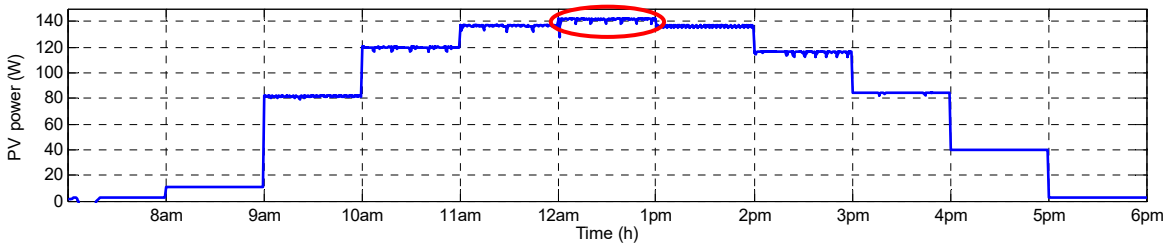

Figure 11-a: PV power variation- IC.

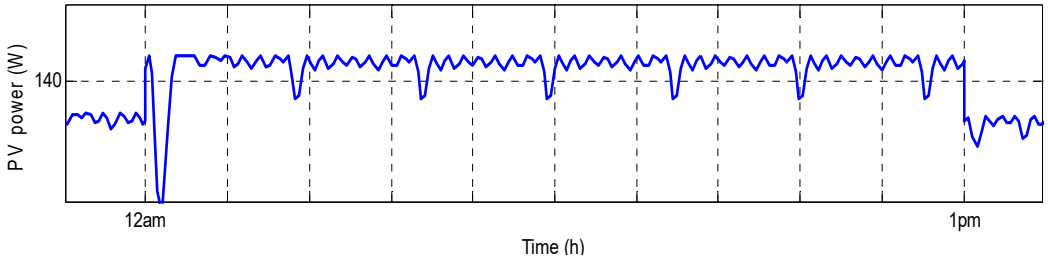

Figure 11-b: PV power variation- IC - zoom.

Fig. 12-a shows the output power of the PV module with robust MPPT scheme. It can be deducted from the curve that the power supplied by the PV module to charge the battery through the converter varies accordingly to the solar radiation and the temperature of the environment. So, the use of the BS MPPT technique provides good performance in tracking the MPP and without oscillations around it (Fig. 12-b) compared to the conventional IC one, which reduces the energy losses.

Fig. 13 shows the duty cycle waveform of the boost converter controlled by the IC MPPT technique, under the influence of solar radiation and temperature variations. It is clearly observed that the variation of the duty cycle pursue the changes of climatic conditions with considerable oscillations around (Fig. 13-b) its optimal value, which perturb the control of the system.

Fig. 14 shows the duty cycle waveform of the boost converter controlled by the BS controller, under the influence of solar radiation and temperature variations. It can be deducted from the figure that the duty cycle variation pursues perfectly its

ISSN: 1992-8645 www.jatit.org E-ISSN: 1817-3195

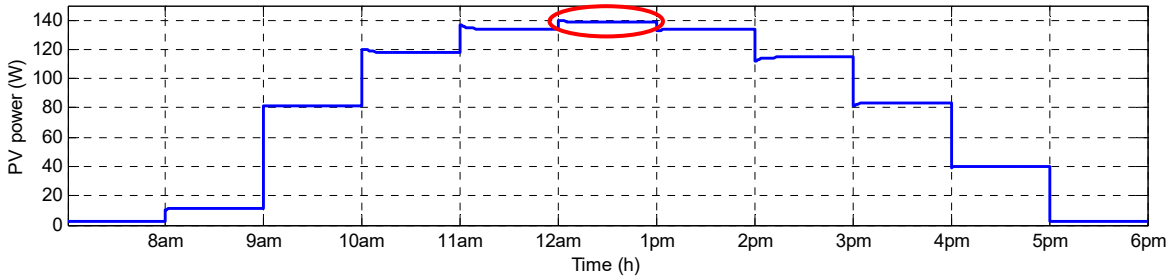

Figure 12-a: PV power variation - BS.

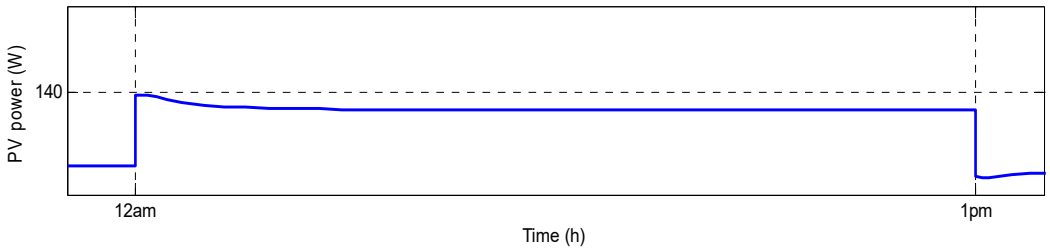

Figure 12-b: PV power variation - BS - zoom.

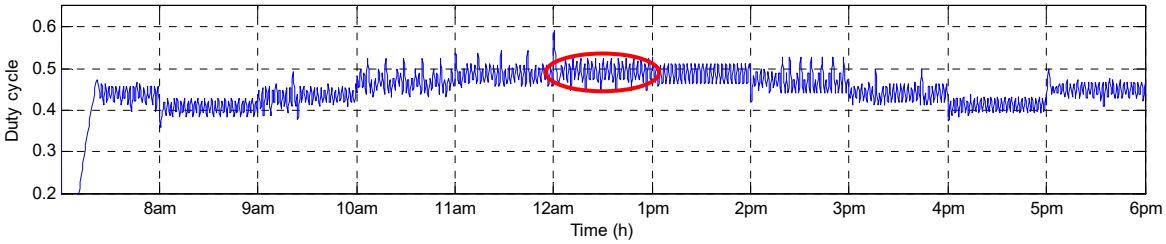

Figure 13-a: Duty cycle variation- IC.

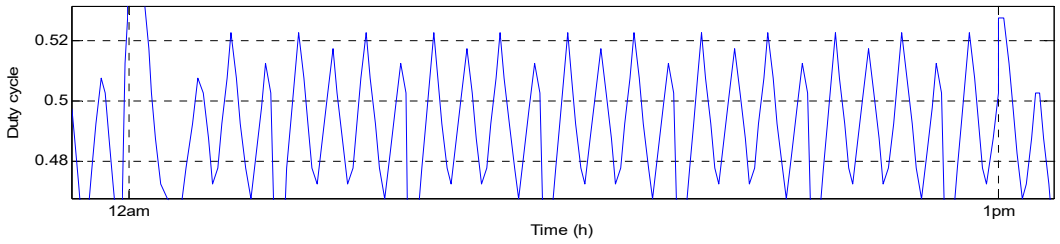

Figure 13-b: Duty cycle variation- IC - zoom.

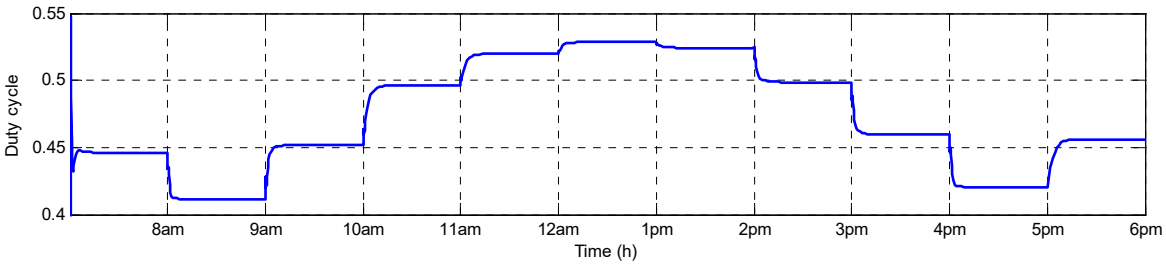

Figure 14-a: Duty cycle variation.

ISSN: 1992-8645 www.jatit.org E-ISSN: 1817-3195

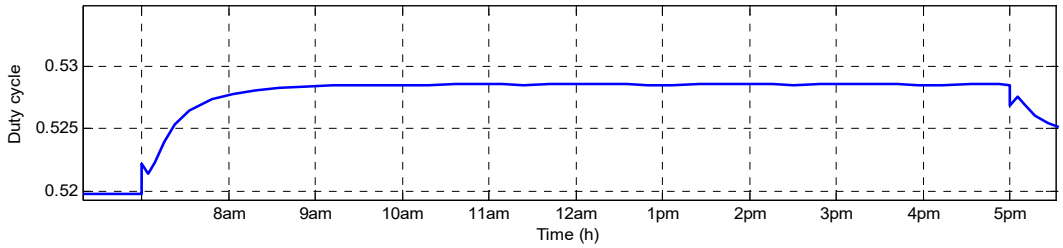

Figure 14-b: Duty cycle variation - zoom.

optimal value without oscillations (Fig. 14-b) compared to that controlled by the conventional IC technique.

Figs. 15 and 16 show current-voltage and power-voltage characteristics and maximum power point (MPP) for different solar radiation and temperature levels for the monocristalline PV module, using the Incremental Conductance MPPT technique.

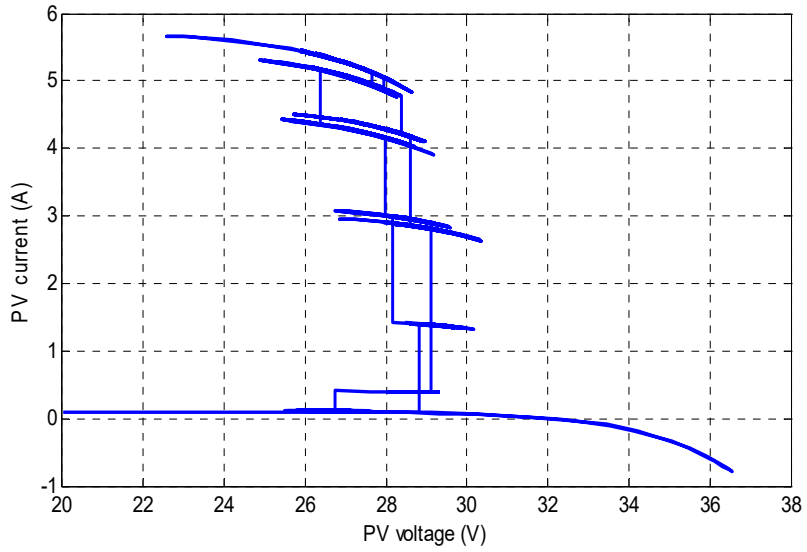

Figure 15: Characteristic curves current-voltage at different solar radiation and temperature levels - IC.

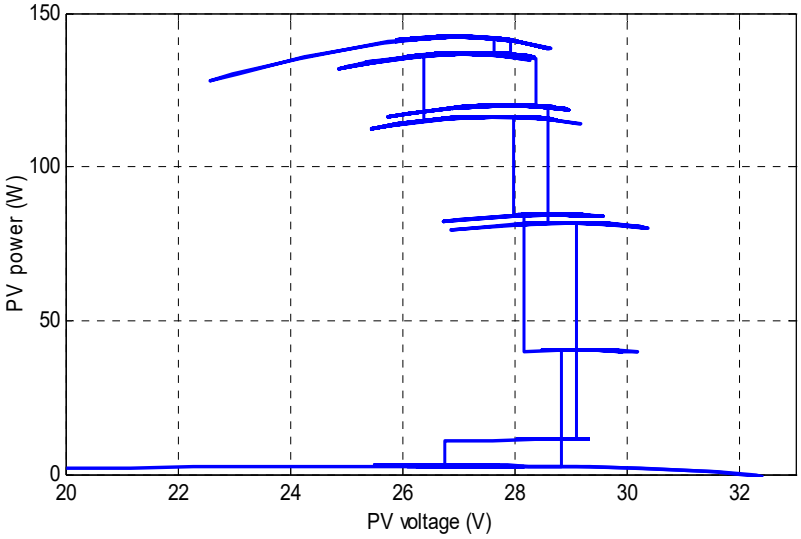

Figure 16: Characteristic curves power-voltage at different solar radiation and temperature levels - IC.

ISSN: 1992-8645 www.jatit.org E-ISSN: 1817-3195

Figs. 17 and 18 show current-voltage and power-voltage characteristics and maximum power point (MPP) for different solar radiation and temperature levels for the monocristalline PV module, using the Backstepping MPPT technique.

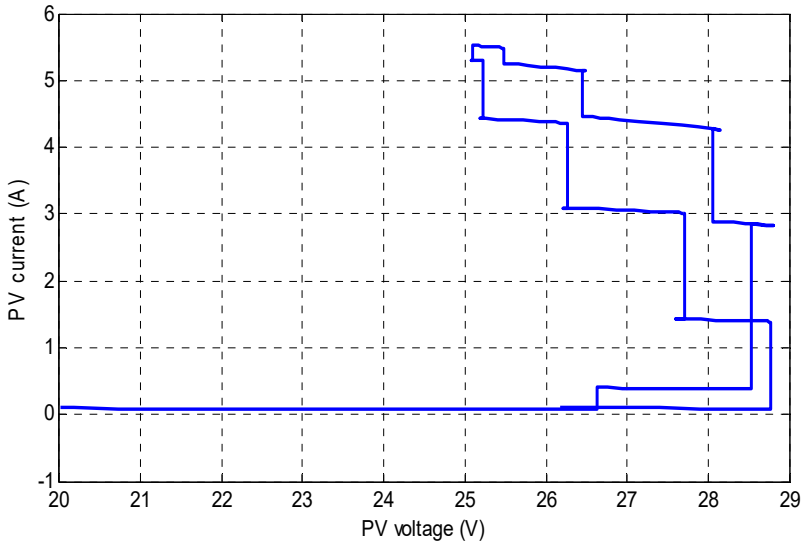

Figure 17: Characteristic curves current-voltage at different solar radiation and temperature levels - BS.

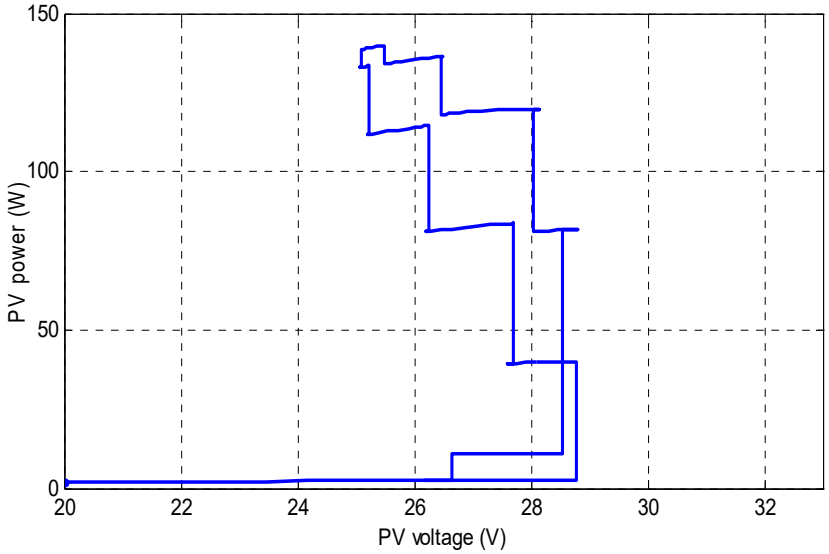

Figure 18: Characteristic curves power-voltage at different solar radiation and temperature levels - BS.

It can be noted that the MPP is always achieved after a smooth transient response without oscillations for the BS MPPT controller (Figs. 17 and 18) and with oscillations for the IC MPPT controller (Figs. 15 and 16). This way, the validation of the robustness of the proposed backstepping controller in presence of solar radiation and temperature variations is guaranteed.

Fig. 19 shows the evolution of the controller output y. When the maximum power is reached, the controlled output $y=dP/dV$ converges to zero.

ISSN: 1992-8645 www.jatit.org E-ISSN: 1817-3195

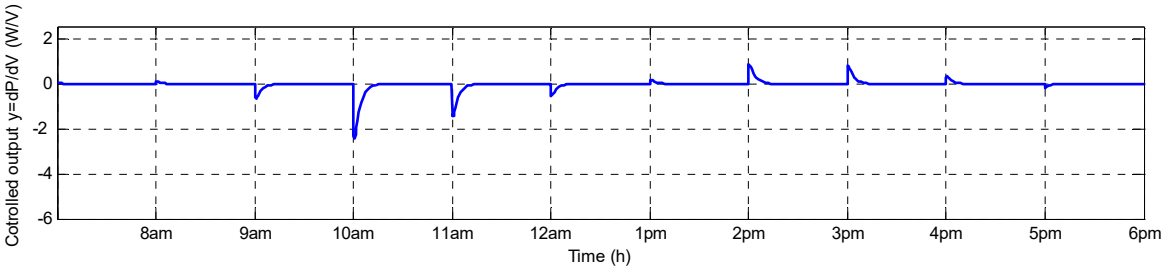

Figure 19: Varying of controlled output y.

6. CONCLUSION AND FUTURE WORK

In this paper, a MPPT controller of standalone PV system using a non-linear backstepping algorithm has been proposed. The subject controller is designed to track the MPP of a Monocristalline PV module. This latter is connected to a DC load through a boost DC-DC converter. The whole system has been simulated using Matlab/Simulink environment. Good performance control of battery charging is achieved using the backstepping control based on tracking errors and asymptotic stability which has been proved using Lyapunov stability criteria.
The simulation results showed that, in comparison with the conventional incremental conductance controller, the proposed controller admits a good performance against variations of real measurements of solar radiation and temperature. From these comparisons, it is clear that the designed controller approach is more robust, stable and accurate than the conventional one.

Future work will contribute to first development of a similar studied system on another platform, i.e. the programmable logic controller (PLC) type Siemens. The entire PV system will be modeled using the SIMATIC TIA Portal software and the PLC HMI. The simulations will be performed using parameters currently considered in literature to show the robustness of the backstepping algorithm for MPPT and its workability under variants whether conditions through automation PLC for industrial purposes.

REFRENCES:

[1] Fattori, F., Anglani, N., Muliere, G., 2014. Combining photovoltaic energy with electric vehicles, smart charging and vehicle-to-grid. *Solar Energy* 110, 438–451.

[2] Rasool, M., Mojallizadeh, Badamchizadeh, M., Khanmohammadi, S., Sabahi, M., 2016. Designing a new robust sliding mode controller for maximum power point tracking of photovoltaic cells. *Solar Energy* 132, 538-546.

[3] Hamrouni, N., Jraidi, M., Cherif, A., 2009. Theoretical and experimental analysis of the behavior of a photovoltaic pumping system. Solar Energy 83, 1335-1344.

[4] Wadgy, R., Anis, M., Abdul-Sadek, N., 1994. Switching mode photovoltaic pumping system. *Journal of Power Sources* 47, 35-43.

[5] Yatimi, H., Ouberri, Y., Aroudam, E., 2019. Enhancement of power production of an autonomous PV system based on robust MPPT technique. *Procedia Manufacturing* 32, 397-404.

[6] Yatimi, H., Aroudam, E., 2018. Algorithms based modeling and control for photovoltaic system under variable climatic conditions. *Procedia Manufacturing* 22, 757-764.

[7] Ahmed, J., Salman, Z., 2015. An improved perturb and observe (p&o) maximum power tracking (MPPT) algorithm for higher efficiency. *Applied Energy* 150, 97-108.

[8] Li, S.,Liao, H., Yuan, H., Ai, Q., Chen, K., 2017. A MPPT strategy with variable weather parameters through analyzing the effect of the DC/DC converter to the MPP of PV system. *Solar Energy* 144, 175-184.

[9] Jubaer, A., Zainal, S., 2015. An improved perturb and observe (P&O) maximum power point tracking (MPPT) algorithm for higher efficiency. *Applied Energy* 150, 97 – 108.

[10] Piegari, L., Rizzo, R., 2010. Adaptive perturb and observe algorithm for photovoltaic maximum power point tracking. *Renew Power Generation*, IET 4, 317–28.

[11] Zhang, F., Thanapalan, K., Procter, A., Carr, S., Maddy, J., 2013. Adaptive hybrid maximum power point tracking method for a photovoltaic system. *Energy Conversion, IEEE Trans* 28, 353–60.

ISSN: 1992-8645 www.jatit.org E-ISSN: 1817-3195

[12] Xiao, W, Dunford, WG., 2004. A modified adaptive hill climbing MPPT method for photovoltaic power systems. *Power Electronics Specialists Conference, PESC 04 2004 IEEE 35th Annual*, 1957–63.

[13] Ahmed, E.M., Shoyama, M., 2011. Stability study of variable step size incremental conductance/impedance MPPT for PV systems. *In: IEEE 8th International Conference on Power Electronics and ECCE Asia* (ICPE & ECCE), 386–392.

[14] Mujahed, A., Ahmed, M. N., Hegazy, R., Kottakkaran, S. N., 2018. Optimal parameter design of fractional order control based INC-MPPT for PV system. *Solar Energy* 159, 650-664.

[15] Kok Soon Tey, Saad Mekhilef, 2014. Modified incremental conductance MPPT algorithm to mitigate inaccurate responses under fast-changing solar irradiation level. *Solar Energy* 101, 333 – 342.

[16] Tawfik Radjai, Lazhar Rahmani, Saad Mekhilef, Jean Paul Gaubert, 2014. Implementation of a modified incremental conductance MPPT algorithm with direct control based on a fuzzy duty cycle change estimator using dSPACE. *Solar Energy* 110, 325 – 337.

[17] Sid-ali Blaifi, Samir Moulahoum, Rabah Benkercha, Bilal Taghezouit, Abdelhakim Saim, 2018. M5P model tree based fast fuzzy maximum power point tracker. *Solar Energy* 163, 405–424.

[18] N. Ammasai Gounden, Sabitha Ann Peter, Himaja Nallandula, S. Krithiga, 2009. Fuzzy logic controller with MPPT using line-commutated inverter for three-phase grid-connected photovoltaic systems. *Renewable Energy* 34, 909 – 915.

[19] N. Patcharaprakiti and S. Premrudeechacharn, 2002. Maximum Power Point Tracking Using Adaptive Fuzzy Logic Control for Grid-Connected Photovoltaic System. IEEE, 372 – 377.

[20] Rai AK et al., 2011. Simulation model of ANN based maximum power point tracking controller for solar PV system, *Solar Energy* Mater Sol Cells 95(2), 773–778.

[21] Yoash Levron and Doron Shmilovitz, 2013. Maximum Power Point Tracking Employing Sliding Mode Control, *IEEE Trans. on Circuits and Systems* 60 (3), 724-732.

[22] Hanane, Y., Elhassan, A., 2016. Assessment and control of a photovoltaic energy storage system based on the robust sliding mode MPPT controller. *Solar Energy* 139, 557–568.

[23] Yeuness, O., Hanane, Y., Elhassan, A., 2020. Design of a robust sliding mode controller for MPPT based on automation PLC for PV applications. *International Transactions on Electrical Energy Systems* 30, 1–19.

[24] Chen-Chi Chu, Chieh-Li Chen, 2009. Robust maximum power point tracking method for photovoltaic cells: A sliding mode control approach. *Solar Energy* 83, 1370 – 1378.

[25] Fan Liping; Yu Yazhou; Boshnakov, K., "Adaptative Backstepping Based Terminal Sliding Mode Control for DC-DC Convertor", *International Conference on Computer Application and System Modeling* (ICCASM 2010), pp. V9-323-V9-327, 2010.

[26] A. D. Martin and J. R. Vazquez, 2014. Backstepping controller design to track maximum power in photovoltaic systems. *Automatika* 55, no. 1, pp. 22–31.

[27] A. D. Martin, J. R. Vazquez, and R. S. Herrera, "Adaptive backstepping control of a DC-DC converter in photovoltaic systems," *in Proc. IEEE EUROCON*, Jul. 2013, 949–955.

[28] Y. Ouberri, H. Yatimi, and E, Aroudam. Modeling and Simulation of PV Module using Industrial Automation PLC, *ICOA'5: The 5th Annual Conference of the IEEE International conference on optimization and applications, Kenitra, Morocco*, 1-7. DOI: 10.1109/ICOA.2019.8727668 , 2019.

[29] Y. Ouberri, H. Yatimi, and E. Aroudam. Industrial Automation PLC based modeling and diode Ideality factor impact on PV characteristics, *ICCSRE'2019: The 2nd IEEE International Conference of Computer Science and Renewable Energies, Agadir, Morocco,*
DOI**:** 10.1109/ICCSRE.2019.8807632, 2019

[30] Yatimi, H., Ouberri, Y., Chahid, S., Aroudam, E., 2020. Control of an Off-Grid PV system based on the Backstepping MPPT controller. *Procedia Manufacturing* 46, 715-723.

[29] J. Chen, R. Erickson, and D, Maksimovid. Averaged Switch Modeling of Boundary Conduction Mode Dc-to-Dc Converters, *IECON'O1: The 27th Annual Conference of the IEEE Ind. Electronic. Society, Denver, Colorado, USA*, 844-849. DOI 10.1109/IECON.2001.975867, 2001.

ISSN: 1992-8645 www.jatit.org E-ISSN: 1817-3195

[31] Dezhi, Xu, Gang Wang, Wenxu Yan, Xinggang Yan, 2019. A novel adaptive command-filtered backstepping sliding mode control for PV grid-connected system with energy storage. *Solar Energy* 178, 222 – 230.

[32] A. Gupta, Yogesh K. Chauhan, Rupendra K. Pachauri, 2016. A comparative investigation of maximum power point tracking methods for solar PV system. *Solar Energy* 136, 236-253.